Journal of Nonlinear Mathematical Physics Volume 12, Supplement 1 (2005), 1–12 Birthday Issue

# On a "Quasi" Integrable Discrete Eckhaus Equation

*M J ABLOWITZ* †, *C D AHRENS* †, *and S DE LILLO* ‡,*

† *Department of Applied Mathematics*
*University of Colorado at Boulder, UCB 526*
*Boulder, Colorado 80309-0526*
*E-mail: mark.ablowitz@colorado.edu*

‡ *Istituto Nazionale de Fisica Nucleare*
*Sezione di Perugia, Perugia, Italy*

* *Permenent Address:*
*Dipartimento di Matematica e Informatica*
*Universita di Perugia*
*Via Vanvitelli 1, 06123 Perugia, Italy*
*E-mail: dilillo@pg.infn.it*

*This article is part of the special issue published in honour of Francesco Calogero on the occasion of his 70th birthday*

**Abstract**

In this paper, a discrete version of the Eckhaus equation is introduced. The discretization is obtained by considering a discrete analog of the transformation taking the continuous Eckhaus equation to the continuous linear, free Schrödinger equation. The resulting discrete Eckhaus equation is a nonlinear system of two coupled second-order difference evolution equations. This nonlinear (1+1)-dimensional system is reduced to solving a first-order, ordinary, nonlinear, difference equation. In the real domain, this nonlinear difference equation is effective in reducing the complexity of the discrete Eckhaus equation. But, in the complex domain it is found that the nonlinear difference equation has a nontrivial Julia set and can actually produce chaotic dynamics. Hence, this discrete Eckhaus equation is considered to be "quasi" integrable. The chaotic behavior is numerically demonstrated in the complex plane and it is shown that the discrete Eckhaus equation retains many of the qualitative features of its continuous counterpart.

## 1 Introduction

Discrete nonlinear models play an important role in physics and biology (see for example [5, 13]). Some well known lattices are the Toda lattice [9] and the nonlinear ladder network [10, 11]. This motivated several studies in which integrable discretizations of physically significant PDE's were obtained, such as the nonlinear Schrödinger equation [1, 3], the

Korteweg-de Vries equation [4], and the Sine-Gordon equation [12]. All of the above mentioned studies refer to nonlinear PDE's integrable by the Inverse Scattering Transform (IST); the corresponding discretizations are nonlinear, differential-difference equations, still integrable by the IST method.

In the present contribution, we consider the discretization of a nonlinear Schrödinger-type equation, the Eckhaus equation [7], which belongs to a different class of integrable nonlinear PDE's, often termed C-integrable equations [6]. In fact, the Eckhaus equation is known to be exactly linearized, through a change of dependent variables, into the linear, free Schrödinger equation [7].

The outline of this paper is as follows. First, we obtain a discretization of the Eckhaus equation which is related, via a point transformation, to the (1+1)-dimensional, discrete Schrödinger equation. We show that in the continuum limit the discretization reduces to a system of nonlinear PDE's which is equivalent to the Eckhaus equation. In the large $n$ limit, we can invert the point transformation to obtain an explicit, asymptotic expression for the solution of the discrete model. In general, the point transformation must be evaluated numerically. The results indicate solitonic behavior for the discrete solutions, in analogy with the behavior of the solutions of the continuous model. The novelty here is the following. The continuous Eckhaus equation can be linearized to the linear, (1+1)-dimensional, free Schrödinger equation and both the direct and inverse transformations are explicit. However, for the discrete Eckhaus equation we have only one of the transformations being explicit; namely, the one which takes the nonlinear system to the linear, free Schrödinger equation is explicit. The inverse transformation requires one to solve a first-order, nonlinear, ordinary difference equation, for which no explicit solution is known. Hence, we refer to this discretization as "quasi" integrable. In general, one might even have chaotic dynamics, which we, in fact, find numerically in the complex domain. This is a manifestation of Julia set dynamics. The transformation is found to be effective in the real domain in the sense that numerically solving a first-order nonlinear difference equation is almost immediate. Since the transformation, at a given time $t$, is given by a first-order, ordinary, nonlinear, difference equation, the complexity of solving the full (1+1)-dimensional nonlinear system (2.8) given below is greatly reduced.

## 2 The integrable discrete model

We begin this study with the Eckhaus equation,

$$i\psi_t + \psi_{xx} + 2|\psi|^2_x\psi + |\psi|^4\psi = 0 \tag{2.1}$$

and introduce the linearizing transformation [7]

$$\phi(x,t) = \psi(x,t)\exp\left[\int_{-\infty}^{x} |\psi(x',t)|^2 dx'\right] \tag{2.2a}$$

which is inverted according to

$$\psi(x,t) = \frac{\phi(x,t)}{\left[1 + 2\int_{-\infty}^{x} |\phi(x',t)|^2 dx'\right]^{1/2}}. \tag{2.2b}$$

The transformation (2.2b) maps (2.1) into the linear, (1+1)-dimensional, free Schrödinger equation:

$$i\phi_t + \phi_{xx} = 0. \tag{2.3}$$

Formulas (2.2a) and (2.2b) imply that to every solution $\psi$ of (2.1) there corresponds a solution $\phi$ of (2.3), and vice versa. Moreover, the transformation is explicit. Hence the problem is linearizable and therefore integrable.

In order to obtain an interesting discretization of (2.1), in the following we derive a discretization of (2.3) in order to implement a discrete analogue of the direct transformation (2.2a). To this end, we consider the first-order, (1+1)-dimensional, differential-difference equation

$$i\frac{d\phi_n(t)}{dt} + \frac{\phi_{n+1} + \phi_{n-1} - 2\phi_n}{\epsilon^2} = 0, \tag{2.4}$$

which is a finite-difference, spatial discretization of (2.3). Using the representation

$$\phi_n \equiv \rho_n e^{i\theta_n} \tag{2.5}$$

allows the discrete, linear, (1+1)-dimensional, free Schrödinger equation (2.4) to be written in the equivalent form

$$\rho_{n,t} + \frac{\rho_{n+1}\sin\Delta\theta_n - \rho_{n-1}\sin\Delta\theta_{n-1}}{\epsilon^2} = 0 \tag{2.6a}$$

$$-\rho_n\theta_{n,t} + \frac{\rho_{n+1}\cos\Delta\theta_n + \rho_{n-1}\cos\Delta\theta_{n-1} - 2\rho_n}{\epsilon^2} = 0, \tag{2.6b}$$

where $\Delta\theta_n \equiv \theta_{n+1} - \theta_n$ and $\rho_{n,t} \equiv \frac{d\rho_n(t)}{dt}$, etc. Next, motivated by the continuous transformations (2.2a-b), we introduce the point transformation

$$\rho_n = R_n e^{S_n} \tag{2.7a}$$

$$S_n = \epsilon\sum_{-\infty}^{n} R_j^2, \tag{2.7b}$$

with $R_n \equiv |\psi_n|$, and observe that under (2.7a) and (2.7b), the system (2.6) is transformed into the system

$$R_{n,t} + S_{n,t}R_n + \frac{R_{n+1}e^{\epsilon R_{n+1}^2}\sin\Delta\theta_n - R_{n-1}e^{-\epsilon R_n^2}\sin\Delta\theta_{n-1}}{\epsilon^2} = 0 \tag{2.8a}$$

$$-R_n\theta_{n,t} + \frac{R_{n+1}e^{\epsilon R_{n+1}^2}\cos\Delta\theta_n + R_{n-1}e^{-\epsilon R_n^2}\cos\Delta\theta_{n-1} - 2R_n}{\epsilon^2} = 0. \tag{2.8b}$$

Eqs. (2.8) are a system of first-order, nonlinear, differential-difference equations. In the following we show that they provide a "quasi" integrable discretization of the Eckhaus equation (2.1). To this end, we take the continuum limit of (2.8). In the limit as $n \to \infty$,

$\epsilon \to 0$ with $n\epsilon = x$ finite, we obtain the following relations:

$$R_n \to R \tag{2.9a}$$

$$R_{n\pm1} \to R \pm \epsilon R_x + \frac{1}{2}\epsilon^2 R_{xx} + \cdots \tag{2.9b}$$

$$\theta_{n\pm1} \to \theta \pm \epsilon\theta_x + \frac{1}{2}\epsilon^2\theta_{xx} + \cdots \tag{2.9c}$$

$$S_n = \epsilon \sum_{-\infty}^{n} R_j^2 \to \int_{-\infty}^{x} R^2(x', t)dx', \tag{2.9d}$$

which, when substituted into (2.8), give at $O(1)$ the following system of nonlinear coupled equations:

$$R_t + R\frac{d}{dt}\int_{-\infty}^{x} R^2(x', t)dx' + R\theta_{xx} + 2R_x\theta_x + 2R^3\theta_x = 0 \tag{2.10a}$$

$$-R\theta_t - R\theta_x^2 + R_{xx} + R^5 + 4R^2R_x = 0. \tag{2.10b}$$

The system (2.10) is equivalent to the Eckhaus equation (2.1). To see this, in the linear Schrödinger equation (2.3) we make the substitution

$$\phi = \rho e^{i\theta}, \tag{2.11}$$

which is the continuous analogue of (2.5), and obtain the system

$$\rho_t + 2\rho_x\theta_x + \rho\theta_{xx} = 0 \tag{2.12a}$$

$$-\rho\theta_t + \rho_{xx} - \rho\theta_x^2 = 0. \tag{2.12b}$$

The system (2.12) is equivalent to (2.3). Moreover, by using (2.9c) and $\phi_{n\pm1} = \phi \pm \epsilon\phi_x + \frac{1}{2}\epsilon^2\phi_{xx} + \cdots$, one can verify that (2.12) coincides with the continuum limit of (2.6). We now observe that the direct transformation (2.2a) can be written in the form

$$\rho(x, t) = R(x, t)\exp\left[\int_{-\infty}^{x} R^2(x', t)dx'\right], \tag{2.13}$$

where (2.11) has been used together with the corresponding relation

$$\psi(x, t) = Re^{i\theta}. \tag{2.14}$$

It is now straightforward to verify that under the transformation (2.13), the system (2.12) is mapped into the system (2.10). Thus, we conclude that the system (2.10) is equivalent to the Eckhaus equation (2.1): in fact, it can be obtained, via the direct transformation (2.13), from the system (2.12) which is in turn equivalent to the linear, free Schrödinger equation (2.3). As a consequence, the discrete system (2.8) provides a discretization of the Eckhaus equation (2.1). The system (2.8) is special in the sense that it results from the use of the point transformation (2.7) to the discrete, linear, (1+1)-dimensional, free Schrödinger equation (2.4).

We now show that the point transformation (2.7), in the continuum limit, reduces to the direct transformation (2.2a). From (2.2a), we obtain the following relation for the square modulus of $\phi$ and $\psi$:

$$|\phi(x,t)|^2 = |\psi(x,t)|^2 \exp\left[2\int_{-\infty}^{x} |\psi(x',t)|^2 dx'\right], \tag{2.15}$$

and we stipulate that $\mathrm{Arg}(\phi) = \mathrm{Arg}(\psi)$. On the other hand, from (2.7) we obtain

$$\frac{\rho_n^2}{\rho_{n-1}^2} = \frac{R_n^2}{R_{n-1}^2} \exp\left(2\epsilon R_n^2\right) \tag{2.16}$$

which, when relations (2.9) are used, gives the continuum limit

$$\frac{\rho^2}{\rho^2\left(1-\epsilon\frac{\rho_x^2}{\rho^2}+\cdots\right)} = \frac{R^2\left(1+2\epsilon R^2+\cdots\right)}{R^2\left(1-\epsilon\frac{R_x^2}{R^2}+\cdots\right)}. \tag{2.17}$$

We now use (2.17) together with (2.11) and (2.14) obtaining at $O(\epsilon)$

$$\frac{|\phi(x,t)|_x^2}{|\phi(x,t)|^2} = \frac{|\psi(x,t)|_x^2}{|\psi(x,t)|^2} + 2|\psi(x,t)|^2, \tag{2.18}$$

which in turn implies

$$\frac{\partial}{\partial x}\ln\frac{|\phi(x,t)|^2}{|\psi(x,t)|^2} = 2|\psi(x,t)|^2. \tag{2.19}$$

Finally, integrating (2.19) one obtains exactly (2.15).

Writing $X_n \equiv R_n^2$, (2.16) can be written as

$$X_{n-1} = \frac{\rho_{n-1}^2}{\rho_n^2} X_n e^{2\epsilon X_n}. \tag{2.20}$$

This is an interesting first-order, nonlinear, ordinary, difference equation for $X_n$ and provides the inverse transformation of (2.7). Thus at $t=0$ we use (2.7) to map the initial condition for the discrete Eckhaus equation $\psi_n(t=0) = R_n(t=0)e^{i\theta_n(t=0)}$ to the initial condition for the linear problem (2.4) from (2.5). Note that the phase of the Eckhaus solution is the same as the phase of the linear, free Schrödinger solution. One then solves the linear equation (2.4). However, inversion of the map requires solving a nonlinear, first-order discrete equation, the solution to which, to our knowledge, has no explicit representation. For this reason, we say the discrete Eckhaus equation (2.8) is “quasi” integrable. In Sect. (4), we show that (2.20) yields chaotic-like dynamics (as an analog of the Julia set phenomenon) in the complex plane.

## 2.1 General $l_2$ solution

Here we calculate the general solution of (2.4) with initial data in $l_2$. The initial data $\rho_n(t=0)$, $\theta_n(t=0)$ are obtained from $\psi_n(t=0) = R_n(t=0)e^{i\theta_n(t=0)}$ where $\rho_n$ is obtained from (2.7). Then from the properties of the discrete Fourier transform, we see that the solution of the discrete Eckhaus equation is also in $l_2$ for all time $t$. Using the discrete Fourier transform, the general solution of (2.4) can be written as

$$\phi_n(t) = \frac{\epsilon}{2\pi}\int_{-\pi/\epsilon}^{\pi/\epsilon} \hat{\phi}_0(k) e^{i[kn\epsilon - \omega(k)t]} dk, \tag{2.21}$$

with the transform pair $\phi_n = \frac{1}{2\pi i}\oint \hat{\phi} z^{n-1} dz$, $\hat{\phi}(t) = \sum_{-\infty}^{\infty} \phi(t)_n z^{-n}$, $z = e^{ik\epsilon}$ and the discrete dispersion relation $\omega(k) = \frac{2}{\epsilon^2}[1 - \cos(k\epsilon)]$. Then, using (2.5), (2.21) along with the nonlinear equation (2.16) gives the $l_2$ solution of the discrete Eckhaus equation (2.8). In general, the first-order, nonlinear, ordinary difference equation (2.16) must be inverted numerically. To our knowledge, no explicit expression for the solution is known.

### 2.2 Soliton and asymptotic solutions

In analogy with the continuum case, we expect the discrete Eckhaus equation (2.8) to admit kink-like solutions. In the continuum limit, soliton solutions are obtained from special solutions of (2.3) of the form $\phi = e^{k(x-x_0)-\Omega t}$. We look for similar types of discrete solutions. In fact, one can verify a solution of the discrete Schrödinger equation (2.4) is given by,

$$\phi_n = r^n e^{-\Omega t} e^{i(kn - \omega t)}, \quad r > 1, \tag{2.22a}$$

with

$$\omega = \frac{2 - (r + 1/r)\cos(k)}{\epsilon^2}, \tag{2.22b}$$

$$\Omega = \frac{(r - 1/r)\sin(k)}{\epsilon^2}. \tag{2.22c}$$

The above solution, when used in the transformation (2.20) and using (2.5), gives, at any time $t$,

$$X_{n-1} = \lambda X_n e^{2\epsilon X_n}, \tag{2.23a}$$

where

$$\lambda = \frac{\rho_{n-1}^2}{\rho_n^2} = r^{-2}. \tag{2.23b}$$

Thus, solving (2.23a), using (2.23b), for $X_n(t)$ gives $R_n^2(t)$. With the phase $\theta_n(t) = kn - \omega t$, one obtains the solution to the discrete Eckhaus equation (2.8): $\psi_n(t) = R_n(t)e^{i\theta_n(t)}$. In the continuous limit, (2.15) implies that as $x \to -\infty$, $|\psi|^2 \sim |\phi|^2$, which for a one-soliton solution is of the form $|\psi|^2 \sim e^{2(k(x-x_0)-\Omega t)}$. In analogy with the continuum limit, we now assume $X_n$, for $n \to -\infty$, to have the following form:

$$X_n \approx \frac{C}{r^{2(n-\Omega t)}}, \quad n \to -\infty, \tag{2.24}$$

where $C$ is an arbitrary, non-negative constant and, for convenience, we set $k = 1$. When this is substituted into (2.23), one finds an explicit, asymptotic expression for $X_{n-1}$, which is valid in the large $n$ limit:

$$X_{n-1} \approx \lambda \frac{C}{r^{2(n-\Omega t)}} \exp\left(\frac{2\epsilon C}{r^{2(n-\Omega t)}}\right), \quad n \to -\infty. \tag{2.25}$$

We remark that (2.23) can be viewed as a continuous family (indexed by time $t$) of a discrete dynamical system, with stable fixed points $X_* = 0$ and $X_* = \ln\left(\frac{r^{2k}}{2\epsilon}\right)$.

In the next section, we numerically evaluate the discrete inverse transform (2.20). The results below show that $X_n$ exhibits the expected solitonic (kink-like) behavior.

# 3 Numerical solutions

Here we discuss the numerical inversion of (2.20) and present numerical examples of solitonic-like solutions to the discrete Eckhaus equation. We write (2.20) as

$$X_{n-1} - \lambda_n X_n e^{2\epsilon X_n} = 0, \tag{3.1}$$

where $\lambda_n \equiv (\rho_{n-1}/\rho_n)^2 \geq 0$, $X_n \geq 0$. Appealing to the Implicit Function theorem, we see that given $\lambda_n$ (at time $t$) and $X_{n-1}$, (3.1) is solvable for any $X_n \geq 0$ and by monotonicity the solution is unique. For fixed time $t$, $\lambda_n$ is known from the solution of (2.4). Then, given $X_{n-1}$, we use Newton's method to solve for $X_n$ and hence $R_n = |\psi_n|$. Below we exhibit specific numerical solutions that exhibit solitonic behavior.

## 3.1 Kink-like solutions

Here we display a collision involving two kink-like solutions. First, we discuss the corresponding solution for the continuous Eckhaus equation. We take as a solution to the continuous Schrödinger equation (2.3) the sum of two traveling waves: $\phi = \phi_1 + \phi_2$, with

$$\phi_i(x,t) = A_i \exp\left[p_i\left(x - x_0^{(i)} - \Omega_i t\right)\right] e^{i(k_i x - \omega_i t)}, \quad p_i > 0, \quad i = 1, 2 \tag{3.2}$$

and the dispersion relations $\omega_i = \frac{\Omega_i^2}{4} - p_i^2$, $\Omega_i = 2k_i$. For ease of notation, we define the following quantities:

$$a_i \equiv x - x_0^{(i)} - \Omega_i t, \quad i = 1, 2, \tag{3.3}$$

$$b \equiv (k_1 - k_2)x - (\omega_1 - \omega_2)t. \tag{3.4}$$

Then using (2.2b), the squared modulus of the solution to the continuous Eckhaus equation (2.1) is given by

$$|\psi(x,t)|^2 = \frac{A_1^2 e^{2p_1 a_1} + A_2^2 e^{2p_2 a_2} + 2A_1 A_2 e^{p_1 a_1} e^{p_2 a_2} \cos(b)}{1 + \frac{A_1^2}{p_1} e^{2p_1 a_1} + \frac{A_2^2}{p_2} e^{2p_2 a_2} + \frac{2A_1 A_2 e^{p_1 a_1 + p_2 a_1}}{(p_1+p_2)^2 + (k_1-k_2)^2}\left[(p_1+p_2)\cos(b) + (k_1 - k_2)\sin(b)\right]}. \tag{3.5}$$

In analogy, for the discrete Eckhaus equation, we take as a solution to (2.4) the sum of two traveling waves: $\phi_n = \phi_n^{(1)} + \phi_n^{(2)}$, with

$$\phi_n^{(j)}(t) = r_j^{n-n_0^{(j)}} e^{-\Omega_j t} e^{i(\epsilon k_j n - \omega_j t)} \tag{3.6a}$$

and the discrete dispersion relations

$$\omega_j = \epsilon^{-2}\left[2 - (r_j + 1/r_j)\cos(\epsilon k_j)\right] \tag{3.6b}$$

$$\Omega_j = \epsilon^{-2}\,(r_j - 1/r_j)\sin(\epsilon k_j). \tag{3.6c}$$

To obtain the squared modulus of the discrete Eckhaus equation, we must numerically solve (3.1), as described above. Figure (1) shows a graph of (3.5) for parameter values $A_1 = 1$, $p_1 = 1.2$, $k_1 = 3/4$, $x_0^{(1)} = -20$ and $A_2 = 1$, $p_2 = 1.5$, $k_2 = 1/2$, $x_0^{(2)} = 0$. The figure clearly shows two kink solitons moving to the right, the shorter soliton moving faster than the taller soliton, with a single soliton emerging from the ensuing collision. As noted in [7], the collision is inelastic. Figure (2) shows the corresponding discrete solution for parameter values $r_1 = 1.1$, $n_0^{(1)} = -115$, $k_1 = \pi/2$ and $r_2 = 1.3$, $n_0^{(2)} = -50$, $k_2 = 0.15\pi$. For convenience, we took the lattice spacing $\epsilon$ to be unity. For appropriate values of the

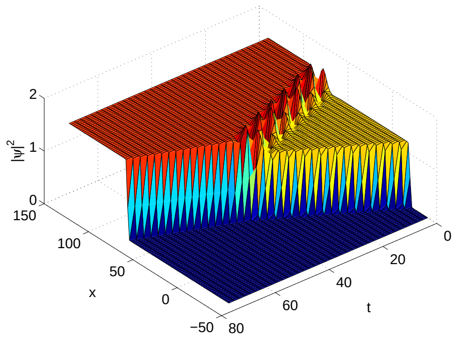


**Figure 1.** Continuous, two-soliton collision

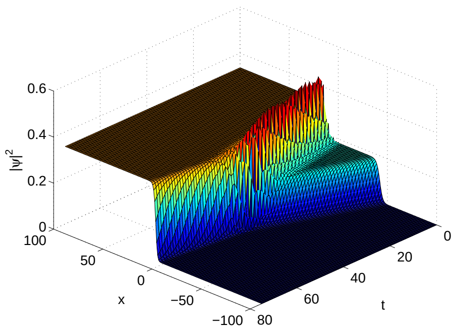


**Figure 2.** Discrete, two-soliton collision

discrete parameters, if we take $\epsilon \to 0$ (i.e. using numerically smaller values of $\epsilon$), the discrete solution is found to converge to the continuous solution. The figures clearly show that the discrete solution is qualitatively similar to the continuous solution.

## 3.2 Boomeron

Here we consider a so-called boomeron [7]. This type of solution arises from a special choice of parameter values in (3.2). Taking $p_1 = p_2 \equiv p > 0$ and $\Omega_1 = -\Omega_2 \equiv \Omega > 0$, (3.5) reduces to

$$|\psi(x,t)|^2 = \frac{A_1^2 e^{2pa_1} + A_2^2 e^{2pa_2} + 2A_1A_2 e^{pa_1} e^{pa_2}\cos(2b)}{1 + +\frac{1}{p}\left[A_1^2 e^{2pa_1} + A_2^2 e^{2pa_2}\right] + \frac{2A_1A_2 e^{pa_1} e^{pa_2}}{p^2+k^2}\left[p\cos(2b) + k\sin(2b)\right]}, \tag{3.7}$$

with $b = kx - \omega t$. As shown in [7], as $t \to -\infty$ there is only one kink moving towards increasing values of $x$ and as $t \to \infty$ there is only one kink moving in the opposite direction, reminiscent of a boomerang. Here we note that in addition to this "boomeranging" feature, the kink emits radiation at the point where it changes direction of travel (see Fig.(3)). (This was previously not noted in [7].) Also, using (3.7) one can show that the radiation persists as $x \to \infty$.

Figure (3) shows a plot of (3.7) for parameter values $A_1 = 1$, $k_1 = 1$, $x_0^{(1)} = -10$, $A_2 = 1$, $k_2 = -1$, $x_0^{(2)} = 10$, $p = 1.5$ and $\Omega = 2$, while Fig. (4) is the corresponding discrete solution

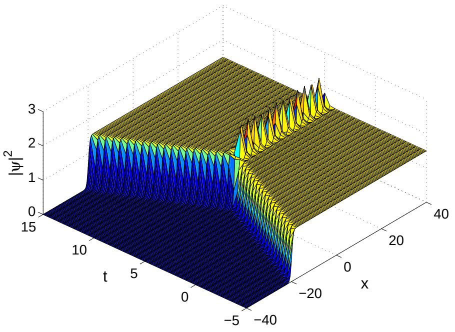


**Figure 3.** A continuous boomeron

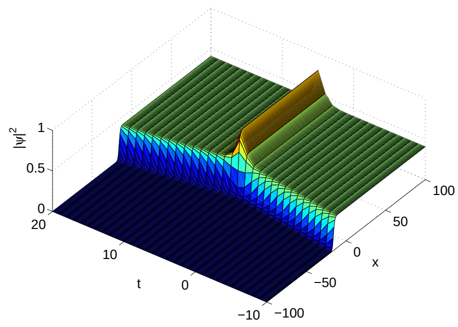


**Figure 4.** A discrete boomeron

with parameter values $r = 1.5$, $n_0^{(1)} = -10$, $k_1 = \pi/2$, $n_0^{(2)} = 10$, $k_2 = \pi/2$. Again, the figures show that the discrete solution retains the qualitative features of the continuous solution, even for $\epsilon = 1$. When $\epsilon$ is sufficiently reduced, the discrete solution tends to its continuous counterpart.

## 4 Chaotic dynamics

The singularity structure in the complex plane of a solution to a difference equation is intimately related to the integrability of the equation [2]. To investigate the map (3.1), we extend (3.1) to the complex plane by allowing $X_n$ to be complex valued, now denoted by $Z_n$. Because of the utility of Newton's method in numerically solving (3.1), we first consider the Newton map associated with (3.1), given by

$$Z_{n+1} = Z_n - \frac{f(Z_n)}{f'(Z_n)}, \tag{4.1}$$

where $f(Z) = \alpha - \lambda Z e^{2\epsilon Z}$. We take $\lambda$ to be independent of $n$, for simplicity. More explicitly,

$$Z_{n+1} = \frac{2\epsilon Z_n^2}{1 + 2\epsilon Z_n} + \frac{\alpha e^{-2\epsilon Z_n}}{\lambda(1 + 2\epsilon Z_n)}. \tag{4.2}$$

Note that here $n$ is an iteration index and not a spatial index as in (3.1). The idea is to now vary $\alpha$ in the complex plane (which is analogous to varying $X_{n-1}$ in (3.1)) and determine which values of $\alpha$ render (4.2) a convergent sequence and which do not. In this way, we obtain the filled Julia-like set associated with the Newton map (4.2). Numerically, for a fixed $\alpha$, if the sequence (4.2) did not converge in 100 iterations, it was deemed divergent. Figure (5) shows the resulting calculation. (See next page.)

Black regions are divergent, while white regions are convergent. For simplicity, we took $\epsilon$ and $\lambda$ to be unity and used a starting iterate of $Z_0 = 1$. Moving from left-to-right, top-to-bottom, the figures are magnified by roughly a factor of ten. The figures clearly

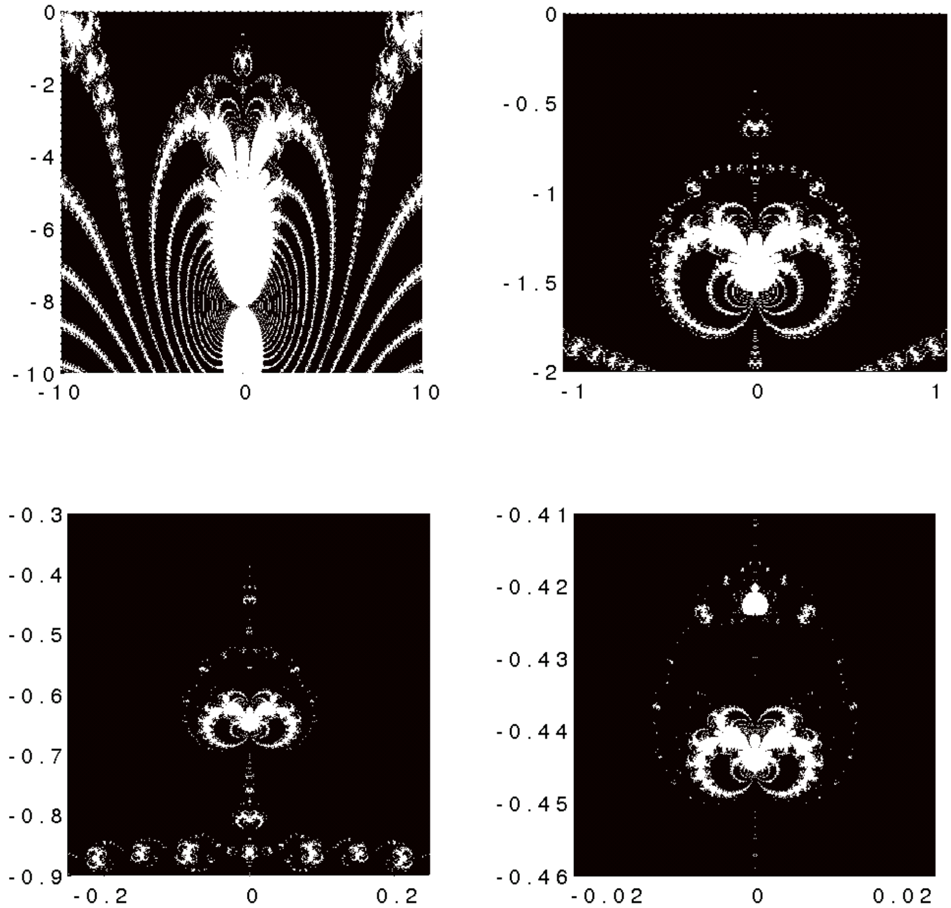


**Figure 5.** Fractal-like structure generated by Newton map associated with $f(z) = \alpha - ze^{2z}$. Black regions are divergent and white regions convergent.

show a self-similar structure, indicative of a fractal on the boundary of the filled Julia-like set. This strongly suggests that there are regions in the complex $\alpha$ plane where (4.2) has chaotic dynamics. This complicated structure indicates that the discrete Eckhaus equation in not integrable because it is obtained by employing the chaotic map (2.20). Here we have used the term quasi-integrable. We note that the filled Julia-like set obtains in the limit as $n \to \infty$. This relates to the behavior of the transformation (4.2) in the sense of reference [2], which investigates the growth properties of the solution as $|n| \to \infty$ with $n$ complex.

We finally remark that the original map $f(z) = \lambda z e^{2\epsilon z}$ numerically demonstrates chaotic dynamics as well. Figure (6) shows the filled Julia set for this map. For convenience, we took $\epsilon = 1/2$ and $\lambda = 1$. The figures were generated by sampling the complex $z$ plane for a

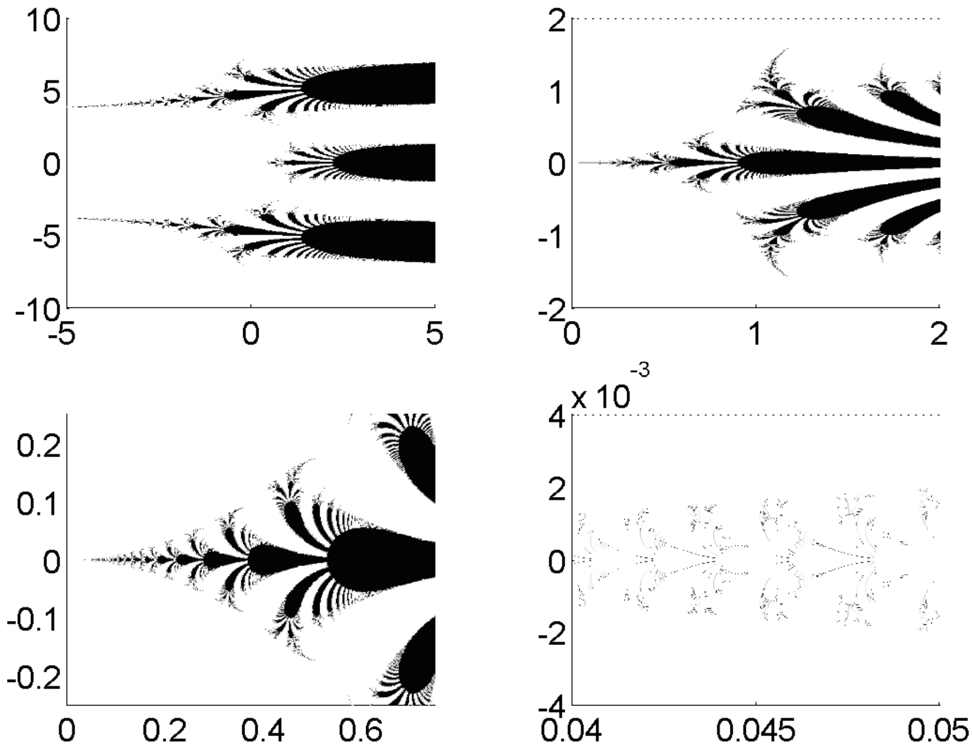


**Figure 6.** Filled Julia set generated by $f(z) = ze^z$. Black regions correspond to numerically unbounded orbits, while white regions correspond to numerically bounded orbits.

starting iterate $z_0$; this point was then iterated 30 times according to $z_{n+1} = f(z_n) = z_n e^{z_n}$. If for any $n$ $\mathrm{Re}(z_n) > 20$, then the point $z_0$ was considered to have an unbounded orbit, i.e., numerically $|z_n| \to \infty$. Also if $|z_{30}| > 10$ the point was considered to have an unbounded orbit, but if $|z_{30}| < 10$ the point was considered to have a bounded orbit. The structure in Fig. (6) was insensitive to the arbitrarily chosen bounds of 10 and 20. These dynamics appear to be similar to those generated by $f(z) = e^z$, which has been shown to have chaotic dynamics [8]. We stress that on the real line neither the original map $f(z) = \lambda z e^{2\epsilon z}$ nor the Newton's-method map (4.2) exhibit chaotic dynamics; it is only when extended to the complex plan that we numerically observe the chaotic behavior.

## 5 Conclusion

In this paper, we have introduced a discrete version of the Eckhaus equation by discretizing the transformation taking the continuous Eckhaus equation to the linear, (1+1)-dimensional, free Schrödinger equation. We showed that in the continuum limit, the discrete Eckhaus equation reduces to the continuous version. The discrete Eckhaus introduced here is a coupled system of two, (1+1)-dimensional, second-order, ordinary, difference, nonlinear evolution equations. However, the system is reduced to a nonlinear, first-order, difference equation, greatly reducing the complexity of the problem. Since this equation does not have a known explicit solution, we refer to this discrete Eckhaus equation as "quasi" integrable, and moreover when the first-order difference equation is extended to the complex plane, we numerically demonstrated that there are regions of chaotic dynamics. Such lower dimensional reductions might be useful in understanding and reducing the difficulty of a much wider variety of nonlinear equations.

## 6 Acknowledgments:

This work was partially supported by NSF grants DMS 0303756 and DMS 9810751.

## References

[1] M.J. Ablowitz and J.F. Ladik, Nonlinear differential-difference equations, *J. Math. Phys.* **16**, 598 (1975).
M.J. Ablowitz and J.F. Ladik, Nonlinear differential-difference equations and Fourier analysis, *J. Math. Phys.* **17**, 1011 (1976).

[2] M.J. Ablowitz, R. Halburd, and B. Herbst, On the extension of the Painlevé property to difference equations, *Nonlinearity* **13**, 889 (2000).

[3] T.R. Taha and M.J. Ablowitz, Analytical and numerical aspects of certain nonlinear evolution equations. II. Numerical, nonlinear Schrödinger equation, *J. Comp. Phys.*, **55**, 203 (1984).

[4] T.R. Taha and M.J. Ablowitz, Analytical and numerical aspects of certain nonlinear evolution equations. III. Numerical, Korteweg-de Vries equation, *J. Comp. Phys.*, **55**, 231 (1984).

[5] M.J. Ablowitz and H. Segur, Solitons and The Inverse Scattering Transform, SIAM Philadelphia (1981).

[6] F. Calogero in: "What is integrability?" edited by V.E. Zakharov, Springer, Berling, pp. 1-62 (1991).

[7] F. Calogero and S. De Lillo, The Eckhaus PDE $i\psi_t + \psi_{xx} + 2(|\psi|^2)_x\psi + |\psi|^4\psi = 0$, *Inverse Problems* **3**, 633 (1987).

[8] R.L. Devaney in: "Complex dynamical systems: the mathematics behind the Mandelbrot and Julia sets," edited by R.L. Devaney, Proceedings of Symposia in Applied Mathematics Vol. 49, AMS, (1994).

[9] H. Flaschka, On the Toda lattice II: inverse scattering solution, *Prog. Theo. Phys.* **51**, (1974).

[10] M. Kac and P. van Moerbeke, On an explicitly soluble system of nonlinear differential equations related to certain Toda lattices, *Advances Math.*, **16**, 160 (1975).

[11] S.V. Manakov, Complete integrability and stochastization of discrete dynamical systems, *Sov. Phys. JETP* **40**, 269 (1975).

[12] L. Pilleni and D. Levi, The inverse scattering transform for solving the discrete sine-Gordon equation, *Phys. Lett.* **92A**, 5 (1982).

[13] Further discretizations of Nonlinear Dynamics in Physical and Biological Systems, Special issue of *Physica D* **68**, (1993).